AIP | Journal of Applied Physics

Theoretical optimization of multi-layer InAs/GaAs quantum dots subject to post-growth thermal annealing for tailoring the photoluminescence emission beyond 1.3μm

K. Ghosh, Y. Naresh, and N. Srichakradhar Reddy

Citation: J. Appl. Phys. **112**, 024315 (2012); doi: 10.1063/1.4739457
View online: http://dx.doi.org/10.1063/1.4739457
View Table of Contents: http://jap.aip.org/resource/1/JAPIAU/v112/i2
Published by the American Institute of Physics.

Theoretical optimization of multi-layer InAs/GaAs quantum dots subject to post-growth thermal annealing for tailoring the photoluminescence emission beyond 1.3 μm

K. Ghosh,[1,a)] Y. Naresh,[2] and N. Srichakradhar Reddy[1]
[1]*School of Electronics Engineering (SENSE), VIT University, Vellore 632014, India*
[2]*Nanotechnology Department, Anna University of Technology, Coimbatore 641047, India*

(Received 14 February 2012; accepted 27 June 2012; published online 24 July 2012)

In this paper, we present theoretical analysis and computation for tuning the ground state (GS) photoluminescence (PL) emission of InAs/GaAs quantum dots (QDs) at telecommunication window of 1.3–1.55 μm by optimizing its height and base dimensions through quantum mechanical concepts. For this purpose, numerical modelling is carried out to calculate the quantized energy states of finite dimensional QDs so as to obtain the GS PL emission at or beyond 1.3 μm. Here, we also explored strain field altering the QD size distribution in multilayer heterostructure along with the changes in the PL spectra, simulation on post growth thermal annealing process which blueshifts the operating wavelength away from the vicinity of 1.3 μm and improvement of optical properties by varying the thickness of GaAs spacing. The results are discussed in detail which will serve as an important information tool for device scientist fabricating high quality semiconductor quantum structures with reduced defects at telecommunication wavelengths. © *2012 American Institute of Physics*. [http://dx.doi.org/10.1063/1.4739457]

I. INTRODUCTION

Recent years witness extensive investigation on self-assembled InAs/GaAs quantum dots (QDs) for optoelectronic devices such as lasers and photodetectors[1–3] due to its unique δ like density of states, size dependent photoluminescence (PL) spectra, low threshold current, and high characteristic temperature. So as to utilize the improved optical properties of QDs in fibre optic communication, a variety of researches were conducted for extending the ground state (GS) PL emission at the high bit rate telecommunication wavelengths of 1.3–1.55 μm.[4–12] Important to mention some of the few researches such as the use of metamorphic buffer layers for efficient emission towards 1.55 μm (Refs. 9–11) as well as 1.4 μm emitters with narrow linewidth.[12] Redshift in the GS PL peak can also be observed in multilayer QD structure which allows to increase in QD size as compared to its single layer counterpart.[13,14] However, this also depends on the strain driven vertical ordering of underlying QDs of varied size distribution which dictates the number density and distribution of the QDs in the upper layers. The major difficulty which arises during the growth of QDs is the dot size inhomogeneity and generation of non-radiative recombination centers as defects, which limit the device performance. Hence, post growth thermal annealing can be carried out which improves QD size homogenization and reduction of structural defects,[15,16] thereby enhancing the device efficiency. However, interdiffusion of gallium and out-diffusion of indium from the QDs on annealing leads to blueshift of the GS PL peak away from the 1.3–1.55 μm region, which impedes the design plan of QD devices applicable for high bit rate optical communication.

In view of the above, we present this paper to provide detailed information to the device scientist about the QD dimensions and distribution which can exhibit longer wavelength PL emission at the telecommunication wavelengths for optical communication as well as reduced blueshifts upon annealing. Here, quantum mechanical models and concepts are used to compute the transition energy state of the QD for different dimensions. To predict the alteration of the QD size in multilayer heterostructure, the size distribution of the QDs is also calculated from lower to upper layers which modify QD bandstructure. The degree of blueshift in the GS PL peak caused by In/Ga interdiffusion at each annealing temperature is also explained and computed using Fick's diffusion model. We further explored the effect of different GaAs spacer thickness on the dot size distribution and emission from the heterostructure.

II. THEORETICAL MODEL

A. Calculation of quantized energy states of InAs/GaAs quantum dots

Three dimensional Schrödinger's equation given by Eq. (1) is solved to obtain the quantized energy states of electrons and holes in the quantum dot using a simple model based on single-band effective-mass approximation

$$\frac{-\hbar^2}{2}\nabla\left(\frac{1}{m^*(r)}\nabla\psi(r)\right)+V(r)\psi(r)=E\psi(r), \qquad (1)$$

Although several well known complex models were reported over the years such as k.p models and pseudopotential method, however, this effective mass approach can be well

a)Author to whom correspondence should be addressed. Electronic mail: kaustab@vit.ac.in.

suited for calculating the ground state energies of the QD in which lays our interest, and it also takes minimum simulation runtime. Since most of the experimental and theoretical works exhibited truncated pyramidal InAs/GaAs QD heterostructure,[17–20] we have used same type of structures in our simulation which was performed using NEXTNANO software.[21] Several researches on quantum dot nanostructures used this particular simulation code to obtain the electron and hole wavefunctions and eigenstates.[22,23] Our simulation is carried out for different QD height and base dimensions with 0.5 nm wetting layer in a simulation box of dimensions (QD base size + 6) × (QD base size + 6) × (QD height + 7) nm^3. The whole simulation area is discretized into grids having 0.5 nm xy in-plane and 0.25 nm vertical grid spacing. NEXTNANO software also includes calculation of strain and Poisson's equation solver to account for the electrostatic interaction energy between the electron and hole charge densities in the QD. The GS PL peak energy of the QD is calculated by

$$E_{PL} = E_{nQDe} + E_g + E_{nQDh}, \tag{2}$$

where E_g is the bandgap of InAs and E_{nQDe} and E_{nQDh} are the ground state energies of electron and holes, respectively, in the QD.

B. Size distribution of quantum dots in multilayer heterostructure

Here, we have assumed sparse array distribution of dot island with an average dot density of 1.5×10^{10} having large spacing between the islands in the first layer of our high misfit (7% misfit between InAs and GaAs) multilayer QD heterostructure. The evolving strain field due to the lattice mismatch from the first layer causes the modification of the QD size distribution in each successive layers of the QD column. This strain in the surface of the embedding QD layer is expressed as[24]

$$\varepsilon(x) = -\varepsilon(L_{dep})[\zeta(1+\zeta^2)^{-3/2}(2+\zeta^2) - \eta(1+\eta^2)^{-3/2}(2+\eta^2)], \tag{3}$$

where $\varepsilon(L_{dep}) = 0.5EL/L_{dep}^2$; E is a coefficient related to misfit and elastic constant of truncated pyramidal QD, and L is QD width. The base centre of the QD is taken as the origin ($x = 0$), $\zeta = (x + L/2)/L_{dep}$, $\eta = (x - L/2)/L_{dep}$, and L_{dep} is the depth of the embedding layer.

Since, the lattice of InAs is greater than GaAs, the region between the QD island becomes compressed (compressive strain) while the regions above the islands expands (tensile strain). The strain given in Eq. (3) is thus the tensile strain above the QD island of the embedded layer. It is assumed that the islands in next layer preferentially nucleate over this tensile region which enhances dot base size and lowers the strain energy by minimizing the misfit between the island and the spacer layer. Hence, the base size of a particular QD in the multilayer depends on the base size distribution and the formation of the tensile area produced by the embedded QDs in the preceding layer. On the average, the

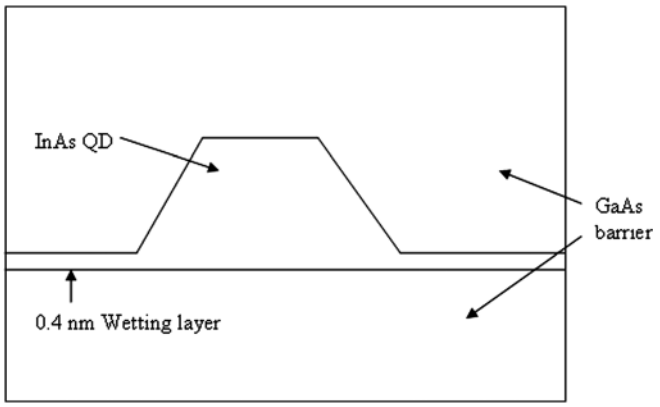

FIG. 1. Sketch of the simulation box containing the InAs/GaAs QD structure.

QD base size L and the tensile region which it produces in a particular layer will bear the same ratio to the summation of all the nucleated QD base size and its total tensile region. The surface strain dependent QD size distribution in a given layer is thus defined as

$$\frac{L_i}{T_{si}} = \frac{L_t}{T_{st}}, \tag{4}$$

where L_i is the base size of the ith layer nucleated QD, $L_t = \sum(L_i)$ is the sum of base sizes of all nucleated QDs, T_{si} is the extent of the ith layer tensile region produced by the nucleated QD structure and $T_{st} = \sum(T_{si})$ is the total tensile area produced by all the buried QD islands.

C. Annealing induced interdiffusion in quantum dots

It is well established that post growth annealing causes In/Ga interdiffusion in the QD structure.[14–16,19,25–27] Simulation is carried out to interpret this interdiffusion process in our optimized QD structures whose operating wavelengths extend to 1.3 μm wavelength as well as the QDs of various

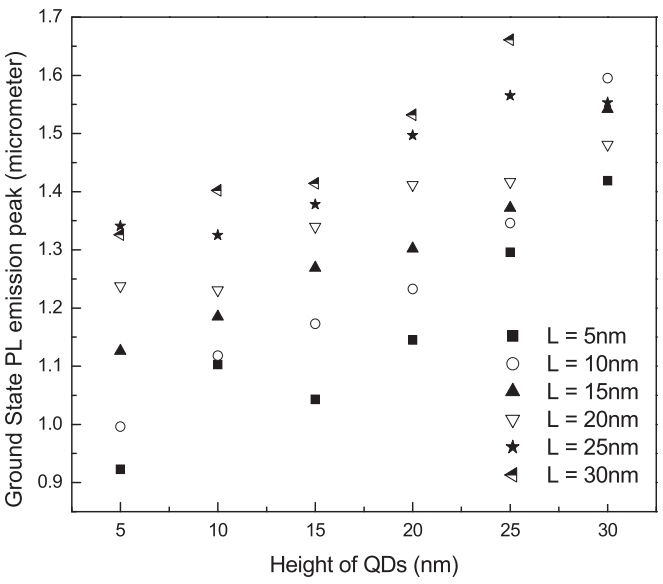

FIG. 2. Computations of the GS PL peak for fixed QD bases with varying heights.

TABLE I. Optimized QD dimensions at which the GS PL emission occurs beyond 1.3 μm wavelength.

QD base (nm)	QD height (nm)	GS PL emission peak (μm)
10	23	1.31
15	20	1.30
20	14	1.32
25	4	1.33

size distributions in the single and multilayer heterostructure. We used Fick's second law of diffusion for the same as given below

$$\frac{\partial x(r,t)}{\partial t} = D\nabla^2 x(r,t), \tag{5}$$

where x(r,t) is the position dependent indium fraction in $In_xGa_{1-x}As$ QD with t duration of the diffusion process and D is diffusion constant of InAs in the QD heterostructure. Here, we have isolated each of the QDs from the distribution and carried out simulation by considering a cuboidal simulation box containing the QD centrally placed as shown in Fig. 1. The box has the dimensions: 3.5 times QD height $\times$ 2 times QD base $\times$ 2 times QD base. We imposed Dirichlet's boundary condition and neglected the coupling and influence of the QDs in the neighbourhood. It is assumed that the QD and the barrier material are purely composed of InAs and GaAs, respectively, and hence we have considered $x = 1$ for asgrown InAs QD material and $x = 0$ for GaAs barrier. To obtain, the In composition of the annealed heterostructure, Eq. (5) is solved in three dimensions by discretization in both time and space with t = 30 s for the annealing time.

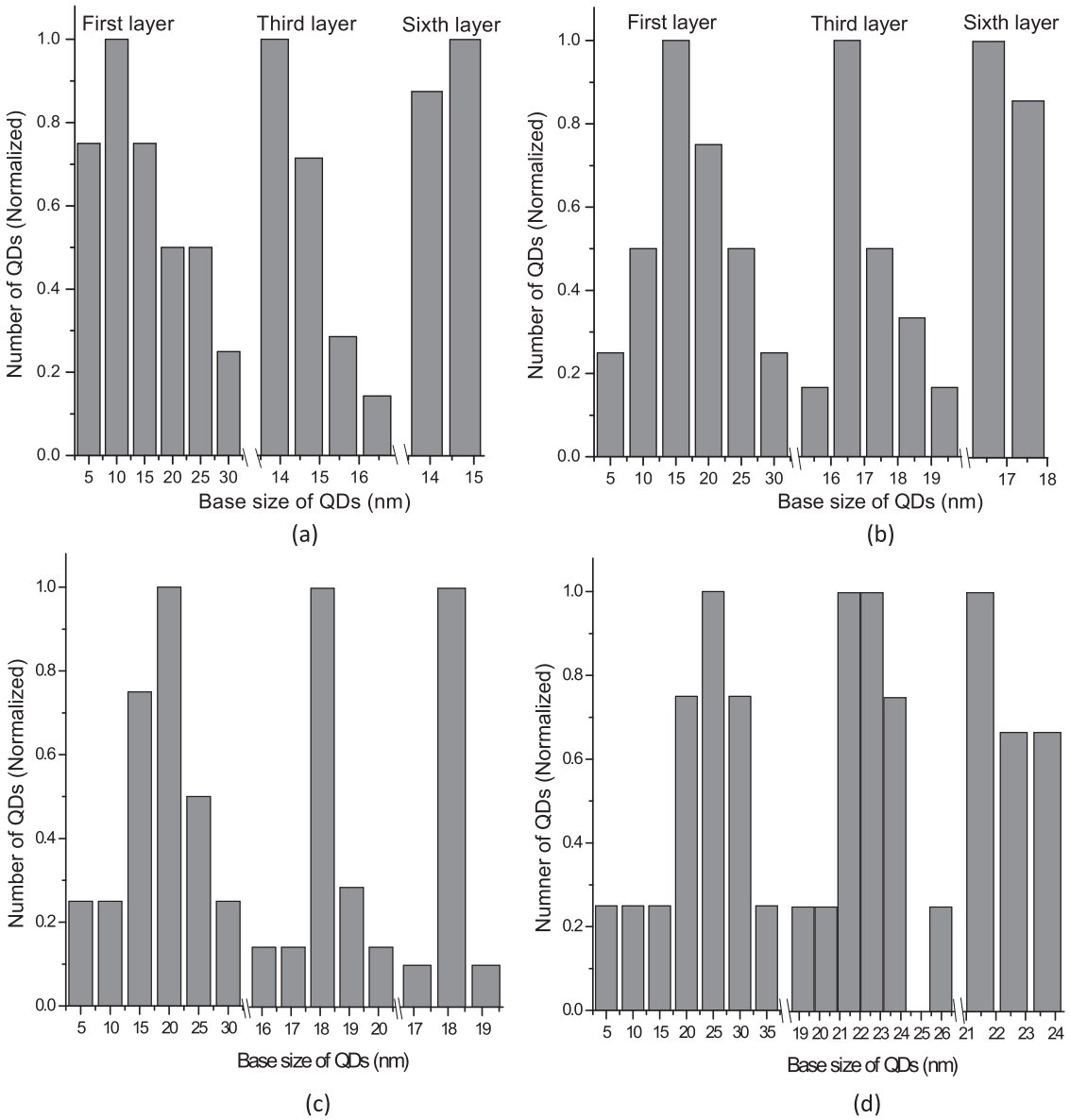

FIG. 3. QD base size distribution in the multilayer heterostructure with (a) A distribution, i.e., maximum number of QDs in the distribution have base width of 10 nm and 23 nm height, (b) B distribution, i.e., maximum number of QDs in the distribution have base width of 15 nm and 20 nm height, (c) C distribution, i.e., maximum number of QDs in the distribution have base width of 20 nm and 14 nm height, and (d) D distribution, i.e., maximum number of QDs in the distribution have base width of 25 nm and 4 nm height, in the first layer.

Arrhenius-type temperature dependence of the diffusion coefficient is taken to account for the variation in properties with annealing temperature T (Ref. 28)

$$D = D_0 \exp\left(-\frac{E_a}{KT}\right), \tag{6}$$

where D_0 is the proportionality constant and E_a is the activation energy of the diffusing species.

In this manner, we obtained asgrown and annealed composition profile of indium for all the QDs of various dimensions in the single and multilayer structure. The position-dependent bulk band gap after interdiffusion is obtained from the following empirical relation involving indium content x in $In_xGa_{1-x}As$ (Ref. 29)

$$E_g = 1.519 - 1.584x + 0.475x^2. \tag{7}$$

III. COMPUTATION AND SIMULATION RESULTS

In this section, we present our computational results. Fig. 2 represents the computations of the GS PL peak for different QD height and base dimensions. Here, we have chosen QD base sizes from 5 nm to 30 nm and varied the QD height. It can be seen that for all fixed base size of QDs, the GS PL peak can be extended to longer wavelength with increase in QD height. The optimized QD dimensions whose GS PL peak emission just reaches the shorter wavelength side of the telecommunication window at 1.3 μm wavelengths is tabulated in Table I. As the computations are done keeping the conditions suitable for minimizing defects and dislocations, we neglected higher QD coverage or larger dimensions for longer wavelength emission near 1.55 μm as it may lead to the nucleation of large sized ripened QDs undergoing strain relaxation through the formation of V-shaped structural defects.[30,31] For the same reason, lower base QD size of 5 nm is not included in Table I as it requires larger height of 26 nm for extending the PL emission to 1.3 μm. We also neglected larger base dimension of 30 nm as it may lead to coalescence with other QD and misfit dislocations.[32]

Fig. 3 shows the base size distribution of single layer, third layer, and sixth layer of the QD heterostructure stack for a typical spacer layer thickness of 10 nm. For the first layer, we have assumed inhomogeneous base-size distribution with the maximum number of QDs having the optimized dimensions given in Table I. These QD size distributions are named as A, B, C, and D, respectively. A distribution is defined as the maximum number of dots in QD assembly having 10 nm base-width and 23 nm height. Similarly, B, C, and D distributions are defined as the maximum number of dots in the assembly having 15 nm base-width and 20 nm height, 20 nm base-width and 14 nm height, and 25 nm base-width and 4 nm height, respectively. The QD aspect ratio and the number density are also considered same for each distribution. The base-size distribution of the upper QD layers is computed through our model. The integration of all the electron transitions arising from single or multilayer QD ensemble having these varied size distribution contributes to the total PL spectra. The

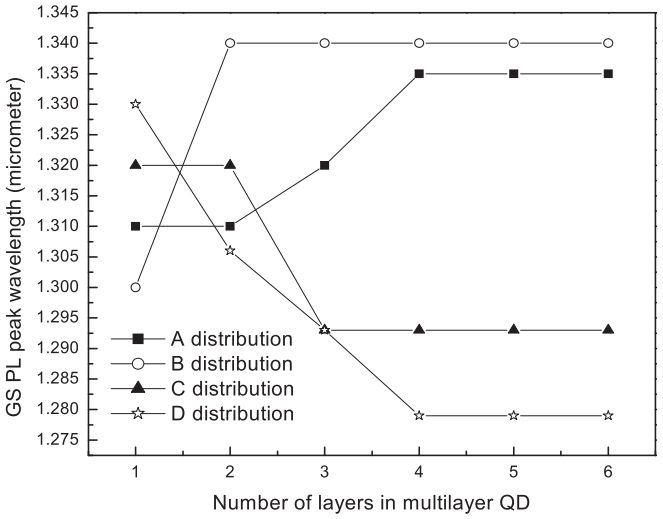

FIG. 4. Computed values of the GS PL peak with increase in the number of QD stacking for A, B, C, and D distributions.

QD having a particular dimension whose number is maximum in the distribution contributes to the most intense PL emission at the corresponding wavelength due to the maximum number of such electronic transitions. Hence, the GS PL peak of the

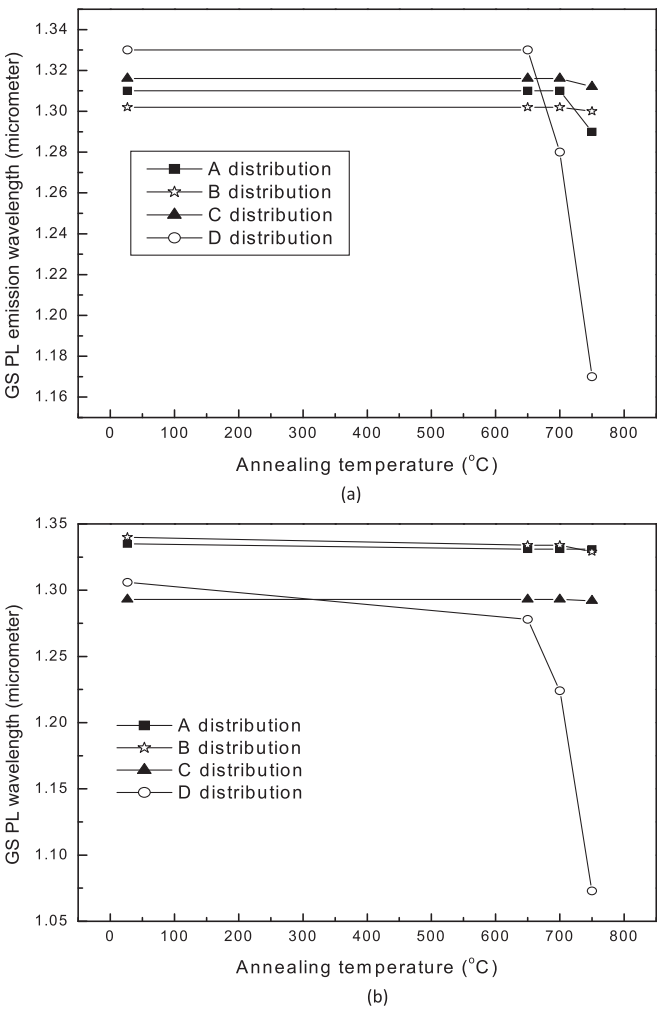

FIG. 5. Computed values of the GS PL peak at different annealing temperatures for (a) A and B distributions for the single layer and its altered distribution in the multilayer (six layer stacking) (b) same for C and D distributions.

PL spectra is the most number of 1-1 electron transitions arising from the QD whose number is utmost in the distribution. This procedure is employed in calculating the GS PL peak for the A, B, C, and D distributions in single layer and its calculated distribution in the multilayer structure. Again coming back to Fig. 3, it can be seen that for all the distributions, the QD base size gradually becomes homogeneous to a narrow range with expansion of the smaller bases and contraction of the larger ones. Our calculations revealed that the smaller QD bases produce larger tensile region above itself as compared to its own base size. Larger tensile area thus causes more expansion of the QD island bases in the succeeding layer. This tensile strain is maximum at the base of the InAs dots over GaAs, which relaxes gradually as it moves towards the periphery. Therefore, we have also taken this into consideration that even though there is increase in QD base size in the succeeding layer, the height remains the same. However, the tensile area produced by larger QDs is not so large as compared to its base width. This slows the QD growth in the successive layers and causes the size to shrink. Since the maximum number of QDs for A distribution has smaller base of 10 nm, its size increases in the succeeding layers. This causes significant red-shifts in the GS PL peak with increase in the number of QD stacking as seen in Fig. 4. This red-shift occurs up to the 4th layer stacking after which it becomes constant due to homogenization of QD size in the upper layers. This is in conformity with other experimental results of multilayer QD exhibiting energy red-shift as compared to single

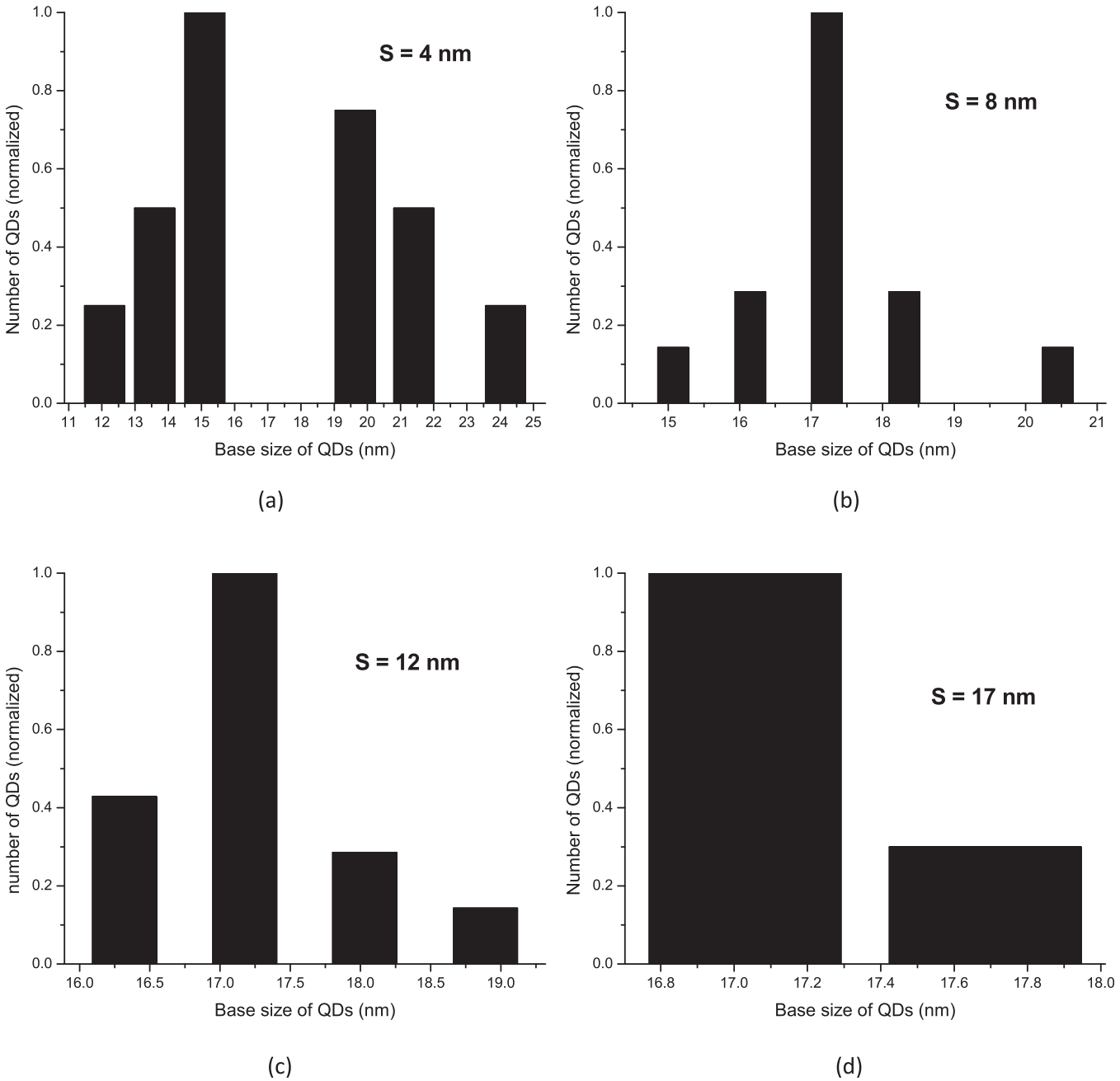

FIG. 6. QD distribution after the third layer stacking of multilayer for GaAs spacer thickness (S) of (a) 4 nm, (b) 8 nm, (c) 12 nm, and (d) 17 nm. The figure depicts that as the spacer thickness is increased, the QD size distribution narrows down to shorter range.

layer sample.[14,33] B distribution has greater number of larger base sized dots than A but lesser than C and D. The tensile strain so produced for B distribution also increases the QD base widths and its number. This causes larger red-shift as compared to A. C and D distributions have maximum number of QDs with larger bases of 20 and 25 nm, respectively. Tensile region produced by these QDs shrinks the size of the succeeding QDs in the upper layers. The tensile region of enlarged QD bases also increases the probability of strain field overlapping with the adjacent QD which may be another reason for shrink in size in the subsequent layers for fixed QD density. This ascribes to the corresponding blueshift in the GS PL peak with increased QD stacking.

Computation on the changes in the GS PL peak on post-growth thermal annealing is carried out for single layer and multilayer structures. Here, we have chosen 650–750 °C annealing temperatures since experiments by other researchers demonstrated that these are the optimized annealing temperatures which reduce non-radiative recombination centers and improve material quality.[15,16] Fig. 5 depicts the blueshift of the GS PL peak for single layer and sixth layer stacked QDs for each of the distributions A, B, C, and D at these annealing temperatures. Notable blueshifts are not seen for A, B, and C distributions in single layer and multilayer structures at each of these annealing temperatures. However, for D distribution, one can observe larger blueshifts with increase in annealing temperatures for both single and multilayer stackings. This may be explained on the basis of traverse area for out-diffusion of indium adatoms from the QDs. Maximum number of QD in A distribution has base size of 10 nm with 23 nm height. This makes larger traverse area for indium adatoms to diffuse out of the QD with increase in anneal temperature, resulting in suppressed blueshift. In the same multilayer structure, the traverse area further increases with increase in QD base which thus causes no alteration in the PL emission wavelength. The same reason ascribes to B and C distributions for single and multilayer heterostructures where maximum number of QDs has base size of 15 nm and 20 nm with 20 nm and 14 nm height, respectively. For D distribution, the QD heights are comparatively much shorter thus decreasing the traverse area for indium. This leads to quicker out-diffusion of indium from the QDs as the annealing temperature is increased causing larger blueshifts.

From all these studies, it can be seen that QDs in A and B distributions show larger red-shift in multilayer stacking and negligible blue-shifts upon annealing. Amongst the two, there are chances of V-shaped defect formation[30,31] due to larger QD height in A distribution. Largest red-shift is seen for B distribution with increased stacking enabling the tuning of the PL emission well above the telecommunication window for effective optical communication. Hence, this B distribution is chosen for studying the effect of spacer layer thickness on optical properties of the QDs. In this respect, a number of researches were conducted to study the effect of spacer layer thickness in improving the optical properties.[34–37] Here, we have assumed initial B distribution of QDs in the first layer and explored the variation of spacer layer thickness on the dot size distribution in successive multilayers. Our intension is to find the optimum spacer

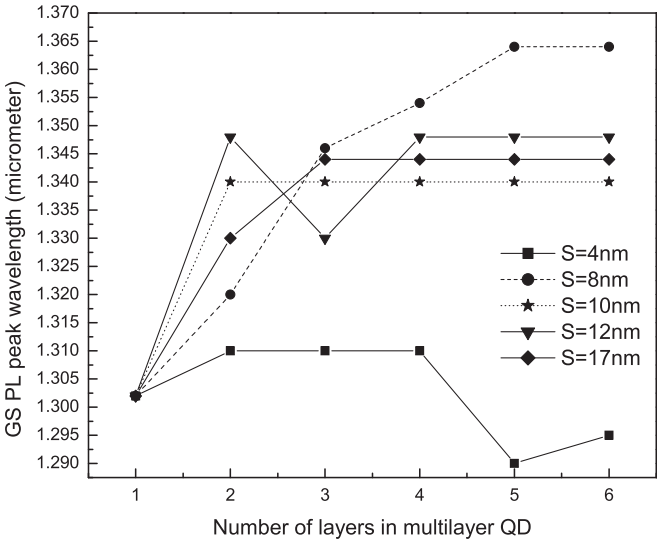

FIG. 7. Degree of GS PL peak blueshift for A, B, C, and D distributions for single layer and multilayer QD (six layer stacking).

thickness of the multilayer heterostructure which can initiate homogenous dot size distribution and extend the PL emission further into the telecommunication window of the near-infrared spectrum. Our calculations revealed that as the spacer layer thickness is increased, the tensile strain above the QDs is also increased. As explained earlier, larger tensile region increases the base widths of smaller QDs and slows the growth or shrinks the size of the larger ones. This causes better homogenization of QD size with increase in spacer thickness. Fig. 6 presents the histogram of dot sizes with different spacer thickness in the third layer of the heterostructure which illustrates our interpretation. By our previously discussed methodology, we also calculated the GS PL emission of the QDs from its size distribution with increase in stacking. Our result is presented in Fig. 7. It is seen that for thinner spacing thickness of 4 nm, there is an initial red-shift of the GS PL peak followed by blue-shift below 1.3 μm after 5th layer stack. However, a larger red-shift is seen with successive stacking for spacer thickness of 8 nm. Further increase in spacer thickness to 10, 12, and 17 nm also causes pronounced red-shift but not as large as caused by 8 nm spacer. This behavior cannot be properly interpreted as this depends on variety of factors such as alteration of QD bases due to tensile strain produced by different spacers, dot density, dot size distribution, dot coalescence, and other factors. However, the dot size homogeneity with 8 nm spacer is not as good as compared to 12 and 17 nm spacers as can be seen from Fig. 6. Thus, although we can have larger extension of PL emission wavelength with 8 nm spacer, we have to compromise with size homogeneity which reduces PL linewidth. In order to have both the aspects, one can suitably choose spacer thickness of 12 or 17 nm or within this range, which can provide better optical property of the QD for its operation in the telecommunication window region.

IV. CONCLUSION

In summary, we presented a theoretical study to calculate the quantized energy states of quantum dots to optimize

the QD dimensions for tuning the PL emission at 1.3 μm. This was followed by the investigation on the QD size distribution in multilayer QD heterostructure. Our computations revealed largest GS PL peak red-shift with multilayer stacking when B distribution (maximum number of dots having 15 nm base-width and 20 nm height in the QD assembly) is chosen in the first layer. Simulation also depicted lesser emission blueshifts for QDs having A, B, and C distributions in single-layer as well as in its multilayer even up to 750 °C annealing. Our computation demonstrated that by choosing B distribution and suitable spacer thickness of 12–17 nm, one can suitably extend the PL emission from the multilayer structure within the telecommunication window along with lower FWHM or linewidth. Our results, thus, provide an important implication for quantum device structures where improved optical quality induced by annealing and optimized GaAs spacer thickness can be effectively utilized for optical communication in 1.3–1.55 μm.

ACKNOWLEDGMENTS

K.G. acknowledges the financial support provided by Department of Science and Technology, Govt. of India.

[1]J. Philips, P. Bhattacharya, S. W. Kennerly, and M. Dutta, IEEE J. Quantum Electron. **35**, 936 (1999).
[2]H. Li, G. T. Liu, P. M. Varangis, T. C. Newell, A. Stintz, B. Fuchs, K. J. Malloy, and L. F. Lester, IEEE Photonics Technol. Lett. **12**, 759 (2000).
[3]W. H. Lin, C. C. Tseng, K. P. Chao, S. C. Mai, S. Y. Lin, and M. C. Yu, IEEE Photonics Technol. Lett. **21**, 1332 (2009).
[4]M. Usman, D. Vasileska, and G. Klimeck, in *Proceedings of the 29th International Conference on the Physics of Semiconductors*, edited by M. J. Caldas and N. Studart (2009), p. 527.
[5]N. Nuntawong, S. Birudavolu, C. P. Hains, S. Huang, H. Xu, and D. L. Huffaker, Appl. Phys. Lett. **85**, 3050 (2004).
[6]M. Usman, S. Heck, E. Clarke, P. Spencer, H. Ryu, R. Murray, and G. Klimeck, J. Appl. Phys. **109**, 104510 (2011).
[7]K. Nishi, H. Saito, S. Sugou, and J. S. Lee, Appl. Phys. Lett. **74**, 1111 (1999).
[8]H. Y. Liu, I. R. Sellers, M. Hopkinson, C. N. Harrison, D. J. Mowbray, and M. S. Skolnick, Appl. Phys. Lett. **83**, 3716 (2003).
[9]H. Y. Liu, Y. Qiu, C. Y. Jin, T. Walther, and A. G. Cullis, Appl. Phys. Lett. **92**, 111906 (2008).
[10]E. S. Semenova, R. Hostein, G. Patriarche, O. Mauguin, L. Largeau, I. Robert-Philip, A. Beveratos, and A. Lemaître, J. Appl. Phys. **103**, 103533 (2008).
[11]L. Seravalli, P. Frigeri, G. Trevisi, and S. Franchi, Appl. Phys. Lett. **92**, 213104 (2008).
[12]E. C. Le Ru, P. Howe, T. S. Jones, and R. Murray, Phys. Rev. B **67**, 165303 (2003).
[13]H. Y. Liu, M. Hopkinson, K. Groom, R. A. Hogg, and D. J. Mowbray, Proc. SPIE **6909**, 690903 (2008).
[14]S. Sengupta, S. Y. Shah, K. Ghosh, N. Halder, and S. Chakrabarti, Appl. Phys. A: Mater. Sci. Process. **103**, 245 (2010).
[15]S. J. Xu, X. C. Wang, S. J. Chua, C. H. Wang, W. J. Fan, J. Jiang, and X. G. Xie, Appl. Phys. Lett. **72**, 3335 (1998).
[16]S. Liang, H. L. Zhu, X. L. Ye, and W. Wang, J. Cryst. Growth **311**, 2281 (2009).
[17]S. Sengupta, N. Halder, S. Chakrabarti, M. Herrera, M. Bonds, and N. D. Browning, Superlattices Microstruct. **46**, 611 (2009).
[18]D. M. Bruls, J. W. A. M. Vugs, P. M. Koenraad, H. W. M. Salemink, J. H. Wolter, M. Hopkinson, M. S. Skolnick, F. Long, and S. P. A. Gill, Appl. Phys. Lett. **81**, 1708 (2002).
[19]M. Srujan, K. Ghosh, S. Sengupta, and S. Chakrabarti, J. Appl. Phys. **107**, 123107 (2010).
[20]H. Shin, J. B. Kim, Y. H. Yoo, W. Lee, E. Yoon, and Y. M. Yu, J. Appl. Phys. **99**, 023521 (2006).
[21]S. Birner, S. Hackenbuchner, M. Sabathil, G. Zandler, J. A. Majewski, T. Andlauer, T. Zibold, R. Morschl, A. Trellakis, and P. Vogl, Acta Phys. Pol. A **110**, 111 (2006).
[22]G. Sarusi, O. Moshe, S. Khatsevich, and D. H. Rich, Phys. Rev. B **75**, 075306 (2007).
[23]O. Moshe, D. H. Rich, B. Damilano, and J. Massies, J. Vac. Sci. Technol. B **28**, C5E25 (2010); Phys. Rev. B **77**, 155322 (2008).
[24]F. Liu, S. E. Davenport, H. M. Evans, and M. G. Lagally, Phys. Rev. Lett. **82**, 2528 (1999).
[25]O. Gunawan, H. S. Djie, and B. S. Ooi, Phys. Rev. B **71**, 205319 (2005).
[26]S. Adhikary, K. Ghosh, S. Chowdhury, N. Halder, and S. Chakrabarti, Mater. Res. Bull. **45**, 1466 (2010).
[27]K. Ghosh, S. Kundu, N. Halder, M. Srujan, S. Sengupta, and S. Chakrabarti, Solid State Commun. **151**, 1394 (2011).
[28]M. Y. Petrov, I. V. Ignatiev, S. V. Poltavtsev, A. Greilich, A. Bauschulte, D. R. Yakovlev, and M. Bayer, Phys. Rev. B **78**, 045315 (2008).
[29]S. Paul, J. B. Roy, and P. K. Basu, J. Appl. Phys. **69**, 827 (1991).
[30]G. Trevisi, L. Seravalli, P. Frigeri, M. Prezioso, J. C. Rimada, E. Gombia, R. Mosca, L. Nasi, C. Bocchi, and S. Franchi, Microelectron. J. **40**, 465 (2009).
[31]P. Frigeri, L. Nasi, M. Prezioso, L. Seravalli, G. Trevisi, E. Gombia, R. Mosca, F. Germini, C. Bocchi, and S. Franchi, J. Appl. Phys. **102**, 083506 (2007).
[32]D. Zhi, M. J. Hytch, R. E. Dunin-Borkowski, P. A. Midgley, B. A. Joyce, and T. S. Jones in *Proceedings on the 14th Conference on Microscopy of Semiconducting Materials, Oxford, United Kingdom, April 11-14, 2005*, edited by A. G. Cullis and J. L. Hutchison (Springer, 2005), pp. 243–246.
[33]J. S. Wang, S. H. Yu, Y. R. Lin, H. H. Lin, C. S. Yang, T. T. Chen, Y. F. Chen, G. W. Shu, J. L. Shen, R. S. Hsiao, J. F. Chen, and J. Y. Chi, Nanotechnology **18**, 15401 (2007).
[34]B. Ilahi, L. Sfaxi, F. Hassen, B. Salem, G. Bremond, O. Marty, L. Bouzaiene, and H. Maaref, Mater. Sci. Eng., C **26**, 374 (2006).
[35]P. B. Joyce, E. C. Le Ru, T. J. Krzyzewski, G. R. Bell, R. Murray, and T. S. Jones, Phys. Rev. B **66**, 075316 (2002).
[36]A. Hospodková, V. Křápek, K. Kuldová, J. Humlíček, E. Hulicius, J. Oswald, J. Pangrác, and J. Zeman, Physica E **36**, 106 (2007).
[37]L. Bouzaiene, B. Ilahi, L. Sfaxi, F. Hassen, H. Maaref, O. Marty, and J. Dazord, Appl. Phys. A: Mater. Sci. Process. **79**, 587 (2004).